**VIS-IR spectral trends in brucite – clay minerals – carbonate mixtures.**

S.De Angelis[1], P.Manzari[1], M.C.De Sanctis[1], E.Ammannito[1,2], T.Di Iorio[1,3] . [1]Istituto di Astrofisica e Planetologia Spaziali, INAF-IAPS, via Fosso del Cavaliere, 100 – 00133, Roma, Italy; [2]University of California Los Angeles, Earth Planetary and Space Sciences, Los Angeles, CA-90095, USA; [3]ENEA SSPT-PROTER-OAC, Roma, Italy.
(simone.deangelis@iaps.inaf.it)

**Introduction.** Carbonates and clay minerals are present in Solar System bodies such as Mars [1] and asteroid Ceres [2,3]. Brucite has been proposed in the recent past to fit absorption features in spectra of Ceres [4]. In this study Visible-Near Infrared reflectance spectroscopic measurements have been performed on brucite-carbonate-clay minerals mixtures, in the 0.2-5.1 μm spectral range. Different sets of three- and two-components mixtures have been prepared using these three fine powdered endmembers, by varying the relative proportions of carbonate, clay and brucite. Spectra have been acquired on the endmembers components separately and on the mixtures. Absorption features diagnostic of the carbonate, clay and brucite phases have been analyzed and band parameters (position, depth, area, width) determined. Several trends and correlations with mineral phase content in each mixture have been investigated, with the aim to determining how endmember components influence the mixture spectra and their minimum detectability threshold.

**Instrument setup.** Analyses have been carried out with the Spectral Imaging (SPIM) facility at INAF-IAPS, Rome. The facility is described in detail in [5,6].
The imaging spectrometer installed in SPIM is a spare of the spectrometer on Dawn spacecraft [7]. It works in the 0.22-5.05 μm spectral range, with a spatial resolution of 38x38 μm on the target. Two bidimensional focal plane arrays, one for the visible between 0.22 and 1.05 μm and one for the IR between 0.95 and 5.05 μm allow to obtaining the spectral coverage. Thanks to the alignment of the bidimensional focal planes with the spectrometer' slit axis (the slit is 9x0.038 mm in size), it is possible to acquire the target's image at different wavelengths.

**Endmembers materials and mixtures description.** Three different end-member samples have been chosen in order to prepare mixtures: (i) a carbonate sample, micritic limestone from Italian Apennines (GPR18); (ii) a clay sample, from Italian Apennines (ML-A-4); (iii) brucite, $Mg(OH)_2$ (commercial). The carbonate and clay were ground and dry sieved, starting from fragments, at a grain size d<20 μm; the brucite was in fine powder form with grain size d>10 μm. Four sets of mixtures have been prepared with different weight proportions: (i) the carbonate proportion is fixed at 10 wt%, while varying the amounts of clay and brucite; (ii) the carbonate proportion is fixed at 40 wt%, while the amounts of clay and brucite are varied; (iii) the carbonate proportion is constant at 70 wt% and the amounts of clay and brucite are then varied; (iv) the fourth set consists of two-components mixtures with no carbonate content.

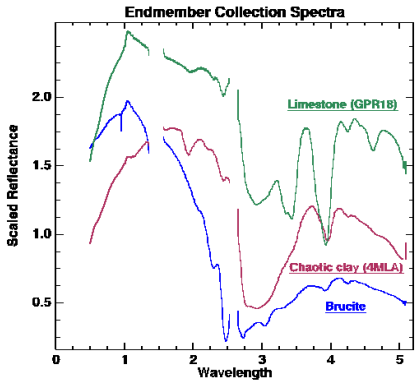


*Fig.1. VIS-IR reflectance spectra of the three endmembers used to prepare the mixtures: micritic limestone (GPR18), chaotic clay (MLA4) and brucite ($Mg(OH)_2$).*

**Analysis and results**. *Endmembers spectra*. The spectra of end-members are in fig.1. The spectrum of the limestone sample (GPR18) is characterized by a weak $H_2O$ absorption near 2 μm, by a broad $H_2O$ feature at 3 μm, and by $CO_3$ absorption bands near 3.4, 3.9 and 4.6 μm. The clay spectrum shows absorption features near 1.9 μm ($H_2O$), two bands at 2.2 and 2.45 μm (Al-OH), a very broad water absorption band at 3 μm, and a $CO_3$ feature at 3.9 μm, indicating that is not a pure sample. Other weak features attributable to some minor $CO_3$ content appear at 3.4 and 4.6 μm. The spectrum of brucite is characterized by the narrow OH absorption appearing at 1 μm and by Mg-OH absorption features occurring at 2.1 and 2.3 μm. The 2.5-μm feature should also be due in principle to Mg-OH, although a filter-artifact in the same spectral region could produce a feature. The water band near 3 μm shows a feature at 2.75 μm (OH) and another one at approximately 3.05 μm, putatively related to strong bonded water [8].
*Mixtures*.
*Mix-1: carbonate content 10 wt%*. The spectra are in fig.2A. The end-member spectra of clay and brucite are also added in the plot. The spectral profiles show several gradual variations as the relative amounts of brucite and clay vary. At high brucite content the narrow OH absorption at 1 μm remains visible (fig.3); the 2.5-μm feature seems to get more deeper as the brucite content increases, suggesting it's real and not related to any artifact (this band has been also reported on the spectra of brucite measured by Beck et al., 2015) [9]. The increasing brucite content also produces a blue more negative slope. The large 3-μm feature tends to flatten and to display a more composite structure. The band at 3.9-μm is due to carbonate in the samples.

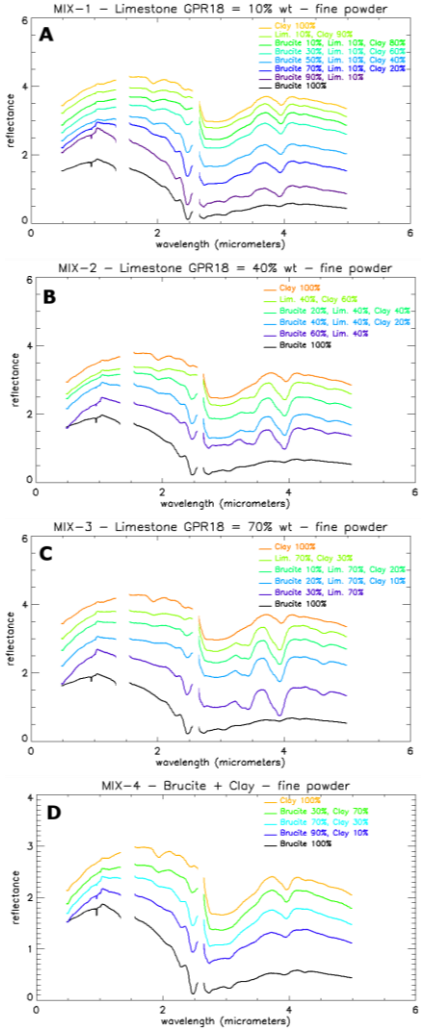


*Fig.2. A: spectra of Mix-1, with carbonate (GPR18) content of 10 wt%. B: spectra of Mix-2, with carbonate content of 40 wt%. C: spectra of Mix-3, with carbonate content of 70 wt%. D: spectra of Mix-4 (no carbonate). Spectra shifted in reflectance for clarity. Instrumental artifacts deleted at 1.4 and 2.5 μm.*

*Mix-2: carbonate content 40 wt%*. At higher carbonate content (fig.2B) the OH 1-μm band is still visible for brucite content higher than 90% (trends in fig.3). The 2.1, 2.3 and 2.5 μm Mg-OH brucite bands tend to increase in strength, while the 1.9-μm $H_2O$ band tends to disappear. All spectra show an increased strength of carbonate 3.4 and 3.9-μm bands, while the 4.6-μm feature is very weak.

*Mix-3: carbonate content 70 wt%*. Spectra in fig.3C. The brucite OH narrow feature at 1 μm is no longer visible in the mixture spectra. The 2.2-μm Al-OH band in clay gradually shifts towards the 2.3-μm Mg-OH band of brucite, as the content of the latter increases; in the same manner the 2.45-μm Al-OH band in clay appears to shift towards the 2.5-μm Mg-OH band of brucite. The spectra are dominated by intense bands of carbonate at 3.4, 3.9 μm, superimposed on the broad $H_2O$ band near 3 μm.

*Mix-4: carbonate content 0 wt%*. The last set consists of two-component mixtures, without carbonate (fig.3D). The 1.9-μm $H_2O$ band of clay is visible for clay content down to 30 wt%; for brucite content of 70 wt% and higher the 2.3-μm Mg-OH band is clearly discernible. The band at 3.9-μm is due to carbonate in the clay.

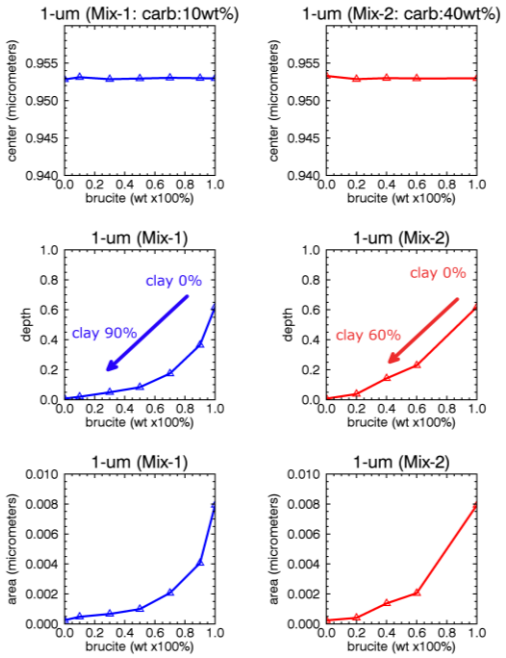


*Fig.3. Band parameters of the 1-μm OH-band of brucite. Parameters are plotted as functions of brucite and clay content, for each fixed value of carbonate in the mixture. Here trends are shown relative to the mixtures MIX-1 and MIX-2.*

**Conclusions.** Analysis of band parameters, such as depths and areas, in mixtures spectra, allowed to identify several trends, and to determine minimum thresholds of detectability of the components. Brucite is recognizable by its narrow OH-absorption at 1 μm, with a minimum 50 wt% content in mixtures containing 10 wt% of carbonate (GPR18), or with a minimum 60 wt% content in mixtures containing 40 wt% of carbonate (GPR18). In mixtures containing 70 wt% of carbonate, this brucite feature is no longer discernible. Finally in two-component brucite-clay mixtures, brucite is recognizable for a minimum content of about 70 wt%. In the analysed mixtures, a high content of brucite is also characterized by very steep blue slope in the 1-2.5 μm range.

**References.** [1] Ehlmann B.L. & Edwards C.S., Ann. Rev. Planet. Space Sci., 42, 291-315, 2014. [2] Rivkin A.S. et al., Icarus, 185, 563-567, 2006. [3] De Sanctis M.C., et al., Lett. Nature, 528, 241-252, 2015. [4] Milliken R.E. & Rivkin A.S., Nat. Geoscience, 2, 258-261, 2009. [5] Coradini A., et al., EPSC Abstracts, EPSC-DPS2011-1043, vol.6, 2001. [6] De Angelis S., et al., Rev. Sci. Instrum., 86, 093101, 2015. [7] De Sanctis M.C., et al., Space Sci. Rev., 163, 329-369, 2011. [8] Frost R.L. & Kloprogge J.T., Spectrochimica Acta Part A 55, 2195–2205, 1999. [9] Beck P. et al., Icarus, 257, 471-476, 2015

**Acknowledgements.** We thanks ASI – Italian Space Agency for supporting this work.